

UC San Diego

UC San Diego Previously Published Works

Title

Inhibition of Neuroinflammation by AIBP: Spinal Effects upon Facilitated Pain States

Permalink

<https://escholarship.org/uc/item/5pk0r868>

Journal

Cell Reports, 23(9)

ISSN

2639-1856

Authors

Woller, Sarah A

Choi, Soo-Ho

An, Eun Jung

et al.

Publication Date

2018-05-01

DOI

10.1016/j.celrep.2018.04.110

Copyright Information

This work is made available under the terms of a Creative Commons Attribution License, available at <https://creativecommons.org/licenses/by/4.0/>

Peer reviewed



Published in final edited form as:

Cell Rep. 2018 May 29; 23(9): 2667–2677. doi:10.1016/j.celrep.2018.04.110.

Inhibition of neuroinflammation by AIBP: Spinal effects upon facilitated pain states

Sarah A. Woller^{#1}, Soo-Ho Choi^{#2}, Eun Jung An³, Hann Low⁴, Dina A. Schneider², Roshni Ramachandran¹, Jungsu Kim², Yun Soo Bae³, Dmitri Sviridov⁴, Maripat Corr², Tony L. Yaksh^{1,#}, and Yury I. Miller^{2,#,&}

¹Department of Anesthesiology, University of California, San Diego, La Jolla, CA;

²Departments of Medicine, University of California, San Diego, La Jolla, CA;

³Department of Life Sciences, Ewha Womans University, Seoul, Korea;

⁴Department of Lipoproteins and Atherosclerosis, Baker Heart and Diabetes Institute, Melbourne, VIC, Australia

These authors contributed equally to this work.

SUMMARY

Apolipoprotein A-I binding protein (AIBP) reduces lipid raft abundance by augmenting removal of excess of cholesterol from the plasma membrane. Here, we report that AIBP prevents and reverses processes associated with neuroinflammatory-mediated spinal nociceptive processing. The mechanism involves AIBP binding to Toll-like-receptor-4 (TLR4) and increased binding of AIBP to activated microglia, which mediates selective regulation of lipid rafts in inflammatory cells. AIBP-mediated lipid raft reductions downregulated LPS-induced TLR4 dimerization, inflammatory signaling and expression of cytokines in microglia. In mice, intrathecal injections of AIBP reduced spinal myeloid cell lipid rafts, TLR4 dimerization, neuroinflammation, and glial activation. Intrathecal AIBP reversed established allodynia in mice in which pain states were induced by the chemotherapeutic cisplatin, intraplantar formalin, or intrathecal LPS, all pro-nociceptive interventions known to be regulated by TLR4 signaling. These findings demonstrate a mechanism by which AIBP regulates neuroinflammation and suggest the therapeutic potential for AIBP in treating preexisting pain states.

&Corresponding author: Yury Miller, yumiller@ucsd.edu, Lead contact: Yury Miller, yumiller@ucsd.edu.

#The Yaksh and Miller laboratories contributed equally to this work

AUTHOR CONTRIBUTIONS

Studies were designed and planned by Y.I.M. and T.L.Y.; experiments were performed by S.A.W., S.-H.C., J.K., D.S., H.L. and E.J.A. Data analysis was performed by S.A.W., S.-H.C. and Y.I.M.; Y.I.M. wrote the manuscript; T.L.Y., M.C., S.A.W., S.-H.C., D.S., R.R. and Y.S.B. contributed to study discussions and manuscript revisions.

DECLARATION OF INTERESTS

The authors declare no competing financial interests. Y.I.M. and T.L.Y. are inventors listed in patent applications related to the topic of this paper.

INTRODUCTION

Apolipoprotein A-I binding protein (AIBP) is a secreted protein discovered in a screen of proteins that physically associate with ApoA-I (Ritter et al., 2002). Human *APOAIBP* mRNA is ubiquitously expressed and the AIBP protein is found in cerebrospinal fluid (CSF) and urine (Ritter et al., 2002) and can be detected in plasma. AIBP has been shown to bind ApoA-I and HDL (Fang et al., 2013; Ritter et al., 2002) and augment cholesterol efflux from endothelial cells and macrophages (Fang et al., 2013; Zhang et al., 2016). Cholesterol efflux regulates the abundance and integrity of lipid rafts, plasma membrane microdomains characterized by a high content of cholesterol and sphingolipids, which serve as functional platforms for the regulation of many surface receptors (Sezgin et al., 2017). Thus, activated Toll-like receptor-4 (TLR4) localizes to lipid rafts and its function critically depends on integrity of rafts, where decreased diffusion rates provide optimal conditions for TLR4 dimerization, an obligatory step in initiation of its signaling cascade (Fessler and Parks, 2011; Schmitz and Orso, 2002; Tall and Yvan-Charvet, 2015). Cholesterol removal from lipid rafts disrupts rafts and consequently inhibits TLR4 signaling (Fessler and Parks, 2011). Therefore, we hypothesized that AIBP-mediated increases in cholesterol efflux should interfere with TLR4-dependent inflammatory signaling.

To address the functional impact of AIBP on TLR4 signaling, we took note of the evolving understanding of the role played by neuraxial TLR4 in regulating the development of facilitated pain states generated by tissue and nerve injury (Park et al., 2014; Saito et al., 2010; Sorge et al., 2011; Stokes et al., 2013b; Woller et al., 2015). TLR4 deficiency in mice prevents the tactile allodynia otherwise evolving over time after afferent activation, as observed with intraplantar formalin (Woller et al., 2016) or as seen with the chemotherapeutic agent cisplatin (Park et al., 2014; Woller et al., 2015). Tellingly, intrathecal (i.t.) injection of LPS, a specific TLR4 ligand, but not of LPS-RS, which does not activate TLR4, results in immediate tactile allodynia (Stokes et al., 2013b). The underlying mechanism involves TLR4-mediated release of inflammatory cytokines from microglia and/or astrocytes, which in turn leads to central sensitization and allodynia (Inoue and Tsuda, 2018; Miller et al., 2015; Stokes et al., 2013b; Sun et al., 2015). We thus believe that the development of neuropathic pain depends at least in part on the release of endogenous TLR4 agonists, such as HMGB1 and HSP70 (Agalave et al., 2014; Feldman et al., 2012; Hutchinson et al., 2009).

Here we demonstrate AIBP binding to TLR4, selective binding of AIBP to activated cells, which results in increased cholesterol efflux and disruption of lipid rafts in inflamed or cholesterol overloaded, but not in non-stimulated cells. In vitro and in vivo in the spinal cord, recombinant AIBP reduced TLR4 dimerization, inflammatory signaling and glial activation. Remarkably, intrathecal delivery of AIBP attenuated persistent facilitated pain states, in the absence of effects upon motor function.

RESULTS

AIBP selectively disrupts lipid rafts in activated microglia and inhibits inflammatory signaling

We hypothesized that AIBP can regulate TLR4 residing in lipid rafts via binding to the receptor and thus recruiting ApoA-I or HDL to TLR4-occupied lipid rafts. Using yeast two-hybrid system, we demonstrated constitutive AIBP binding to the TLR4 ectodomain, but not to ectodomains of TLR1, TLR7 or TLR9 (Fig. 1A and Fig. S1A). At this point, we cannot exclude the possibility of AIBP binding to other TLRs or other cellular receptors. The AIBP-TLR4 binding was confirmed in a pull-down experiment with AIBP and TLR4 ectodomain expressed in HEK 293 cells (Fig. 1B). In addition, recombinant AIBP bound to peritoneal macrophages from wild type (WT) but not *Tlr4*^{-/-} mice (Fig. 1C).

Because TLR4 is involved in glial activation and nociceptive processing and because exposure to LPS results in a greater TLR4 recruitment to lipid rafts, where the receptors dimerize and initiate inflammatory signaling (Wong et al., 2009), we tested whether LPS activation of TLR4 affects AIBP binding to microglia. We found that AIBP binding to BV-2 microglia cells was increased as much as 4-fold following a short stimulation with LPS (Fig. 1D). The finding of LPS-induced increases in AIBP binding to microglia led us to hypothesize that AIBP will selectively target inflamed but not quiescent cells. This is particularly important because exposure to LPS rapidly inhibits cholesterol efflux to gain support to inflammatory signaling (Baranova et al., 2002; Yin et al., 2010). Indeed, we observed that LPS reduced cholesterol efflux from primary microglia and THP-1 macrophages, and AIBP potentiated partial recovery of cholesterol efflux from both cell types stimulated by LPS but did not affect efflux from unstimulated cells (Figs. 1E and F).

To demonstrate that AIBP selectively targets cells under different pathologic conditions, we increased lipid raft abundance by loading macrophages with acetylated LDL (acLDL). AIBP facilitated cholesterol efflux to ApoA-I from acLDL-loaded THP-1 macrophages but not from macrophages with normal cholesterol levels (Fig. 1G). We conclude that AIBP selectively targets inflamed and/or cholesterol overloaded cells but does not affect cells under normal conditions.

The AIBP-stimulated cholesterol efflux was confirmed by measurements of the cholesterol content in a lipid raft fraction of the plasma membrane of BV-2 cells. LPS stimulation increased cholesterol in lipid rafts, and AIBP treatment returned it to basal levels (Fig. 2A). Accordingly, LPS increased the content of cholera toxin B (CTB)-positive lipid rafts in BV-2 cells, and the effect was nullified by AIBP (Fig. 2B). Furthermore, treatment with AIBP reduced LPS-induced TLR4 occupancy in lipid rafts in BV-2 microglia (Fig. 2C). In these and further experiments, we used a dose of AIBP (0.2 µg/ml) previously selected in experiments with endothelial cells and macrophages (Fang et al., 2013; Zhang et al., 2016).

AIBP-mediated cholesterol depletion, disruption of lipid rafts and reduction of TLR4 occupancy in lipid rafts should affect TLR4 activation and signaling. Indeed, AIBP decreased TLR4 dimerization in response to LPS, as was demonstrated in BV-2 microglia (Fig. 2D and Fig. S1B) and in Ba/F3 cells expressing TLR4-flag, TLR4-gfp and MD2 (Fig.

2E). AIBP by itself does not bind LPS (Fig. S2) and is unlikely to affect LPS availability. Treatment with AIBP inhibited downstream effects of TLR4 activation, p65 and ERK1/2 phosphorylation (Fig. 3A and Fig. S3A) and inflammatory cytokine mRNA expression (Fig. 3B and Fig. S3B) in BV-2 microglia in response to LPS. The latter results were replicated in primary mouse microglia in which AIBP completely inhibited LPS-induced expression of the majority of inflammatory cytokines (Fig. 3C). AIBP did not affect cellular cholesterol levels (Fig. S4A).

Spinal AIBP reduces i.t. LPS-evoked TLR4 dimerization, glial activation and CSF cytokines

To examine whether AIBP reduces lipid rafts in spinal cord in vivo, we injected mice i.t. with saline or recombinant AIBP two hours prior to the i.t. injection of LPS. AIBP significantly reduced the abundance of lipid rafts in spinal myeloid cells (including microglia) compared to saline, as was measured ex vivo by CTB binding to CD11b+ cells (Fig. 4A). AIBP-associated lipid raft reductions in spinal myeloid cells in LPS-treated animals averaged 14%, indicating that only a subset of cells, with excessive raft formation, was affected. We hypothesized that this moderate change in membrane microdomain organization has a threshold effect and is sufficient to physiologically inhibit TLR4-mediated neuroinflammation.

Assessment of TLR4 dimerization revealed a uniformly low constitutive presence of TLR4 dimers in naïve (un-injected) mice. In contrast, in the saline/LPS group, TLR4 dimers were uniformly high. As shown, i.t. AIBP pretreatment (AIBP/LPS group) significantly reduced TLR4 dimerization in spinal myeloid cells (Fig. 4B and Fig. S4B). The i.t. saline/saline group was similar to the naïve group but the greater spread likely reflects some degree of activation of TLR4 signaling secondary to the intrathecal needle placement (Stokes et al., 2013b).

Four hours post-injection, i.t. LPS resulted in a highly significant increase in the CSF levels of inflammatory cytokines and chemokines (IL-6, IL-8, CCL2 and CXCL2) as compared to i.t. saline (Fig. 4C). Spinal delivery of AIBP (0.5 µg) significantly reduced LPS-induced expression of inflammatory cytokines in the CSF (Fig. 4C). In addition, examination of GFAP and IBA1, markers of astrocyte and microglial activation, respectively, both revealed significant increases in i.t. LPS treated animals that were also reduced by i.t. AIBP (Figs. 4D and S5). Together, these results suggest that i.t. AIBP inhibits LPS-induced neuroinflammation and glial activation in the spinal cord.

AIBP prevents and reverses facilitated pain states

The pronounced effects of i.t. AIBP on spinal inflammatory signaling prompted consideration of the effects of i.t. AIBP on the expression of several pain states known to be associated with neuraxial TLR4 signaling. *Tlr4* gene knockout or mutant mice are fully protected from tactile allodynia in the models of facilitated pain tested below (Cao et al., 2009; Park et al., 2014; Saito et al., 2010; Sorge et al., 2011; Stokes et al., 2013a; Stokes et al., 2013b; Woller et al., 2015). Accordingly, we addressed the effects of i.t. AIBP at a dose found to alter neuraxial inflammatory cascade in three different mouse models of facilitated processing:

i) i.t. LPS.—As previously reported, male mice injected with i.t. LPS displayed a robust and long lasting tactile allodynia (Stokes et al., 2013b; Woller et al., 2016). While i.t. AIBP and i.t. saline produced minor changes in paw withdrawal thresholds in naïve mice (Fig. S6A), pretreatment with i.t. AIBP, in a dose-dependent manner, significantly prevented i.t. LPS-induced allodynia (Fig. 5A). In contrast, the i.t. injections of saline or denatured, heat-inactivated AIBP displayed no effect upon the i.t. LPS evoked allodynia (Fig. 5A). These studies were also carried out in females. As previously reported, the female i.t. LPS response is significantly reduced compared to males (Woller et al., 2016). However, the initial i.t. injection of AIBP in the female had a discriminable effect profile with a significant reversal in the late versus the early phase (Fig. S6B).

To test the effect of i.t. AIBP in reversing an established pain state, we injected i.t. AIBP 24 hours after i.t. LPS, when the animal showed a severe allodynia. As indicated, the allodynia was markedly attenuated by a single injection of i.t. AIBP, but not of saline (Fig. 5B).

Next, we compared the therapeutic effect of i.t. AIBP in male mice with that of i.t. beta-cyclodextrin (β CD), a class of detergents that solubilize cholesterol (Ohtani et al., 1989). I.t. β CD prevented LPS-induced allodynia for up to 4 hours, but unlike AIBP, β CD at a dose which resulted in a near complete early reversal, was not effective at 24 and 48 hour time points (Fig. 5C). To test if other compounds stimulating physiologic cholesterol efflux pathways have an effect on neuropathic pain, we administered i.t. GW3965, an LXR agonist, which, among other actions, upregulates expression of cholesterol transporters ABCA1 and ABCG1 (Joseph et al., 2003), or i.t. ApoA-I, a cholesterol acceptor. Consistent with the role of lipid rafts and the effects of altering membrane cholesterol, both GW3965 and ApoA-I prevented i.t. LPS-induced tactile allodynia (Fig. 5D and 5E). However, as compared to AIBP, their effects were moderate and transient. These results suggest that the AIBP-augmented turnover of HDL (Fang et al., 2013), targeted to inflamed microglia (Figs. 1 and 2), is a more effective treatment of neuropathic pain, as compared to other means of stimulating cholesterol removal from the plasma membrane.

ii) Intraplantar formalin evoked allodynia.—Intraplantar injection of formalin yields acute biphasic flinching of the injected paw (phase 1 and phase 2). After a 7 day delay, a persistent tactile allodynia progressively develops along with associated activation of spinal microglia (phase 3) (Wu et al., 2004). TLR4 knockout has no effect upon phase 1 or phase 2, but reduces the phase 3 (Woller et al., 2016). In this model, we initially performed i.t. injections of saline or AIBP, followed by intraplantar injection of formalin. Consistent with effects of TLR4 knockout, AIBP had no effect upon phase 1 or 2 formalin-evoked hind paw flinching (Fig. 6A). However, i.t. AIBP given prior to formalin reduced the allodynia otherwise observed on the 7th day after administration of formalin (Fig. 6B).

In separate studies, to determine the effect of AIBP on the established phase 3 allodynia, mice received intraplantar formalin and 7 days later, after development of the allodynia, i.t. AIBP or saline. AIBP but not saline significantly reversed allodynia (Fig. 6C). These results suggest that spinal AIBP inhibits the development of the chronic pain following acute injury and reverses the established allodynia.

iii) Chemotherapy induced tactile allodynia.—Systemic delivery of cisplatin, a chemotherapeutic, results in a robust and enduring tactile allodynia (Park et al., 2013). Here we demonstrate that a single i.t. AIBP injection, administered 4 days after the last cisplatin treatment, completely reversed established allodynia (tactile withdrawal thresholds above 1.0 g are considered normal in this model), with the AIBP therapeutic effect lasting for a minimum of 2 months (Fig. 7A and B).

Intact sensory-motor function in AIBP injected mice

Given the important role lipid rafts play in cell physiology, indiscriminate disruption of lipid rafts may have unforeseen adverse consequences. In a systematic analysis, mice received intrathecal saline or AIBP (0.5 μ g/5 μ L) and were examined without knowledge as to treatment at baseline and 1, 2, 3, and 4 hours and 1, 2, and 7 days after injection. The laboratory gross behavioral inventory assessed arousal, motor function, muscle tone and other end points, as listed in Table S1. As indicated, neither saline nor AIBP produced indices of dysfunction over the 7-day observation interval (Table S1). The placing and stepping reflex reflects the integrity of a spinally mediated plantar placement and spreading of the digits evoked by low threshold (A β) tactile sensitive afferents initiated by dragging the dorsum of the paw across an edge. Many of these measures (except pinnae and blink) are depressed or lost in a dose dependent fashion after i.t. local anesthetics and botulinum toxin (Huang et al., 2011; Penning and Yaksh, 1992). Further we note that animals receiving this dose of i.t. AIBP show little effect upon formalin evoked flinching when delivered in advance of the formalin indicating maintenance of that high frequency hind paw behavior (Fig 6A). These findings uniformly suggest that i.t. AIBP at the dose that has pronounced effects upon aspects of pain processing, has no general effects upon non-nocisponsive behaviors, supporting the selective character of AIBP regulation of lipid rafts in inflamed cells.

DISCUSSION

In this study, we report a mechanism of selective regulation of lipid rafts in activated cells. Cellular studies showed that AIBP bound to activated microglia via TLR4 and augmented cholesterol efflux and disruption of lipid rafts, specifically in stimulated but not unstimulated cells, and reduced TLR4 dimerization. These in vitro properties were confirmed in vivo wherein we showed that direct exposure of spinal cord through i.t. delivery of AIBP prevented: i) i.t. LPS-evoked lipid raft increases; ii) spinal TLR4 dimerization; iii) glial activation as assessed by the expression of microglia and astrocyte markers in spinal cord; and iv) the release of cytokines into the CSF. At the intrathecal dose employed yielding these robust effects upon neuraxial inflammatory cascades, i.t. AIBP resulted in the efficient prevention and reversal of the allodynic effect produced: i) by i.t. LPS; ii) in the late phase (phase 3) intraplantar formalin; and iii) in the polyneuropathy associated with administration of cisplatin, a chemotherapeutic. Comments on issues pertinent to these observations are addressed below.

AIBP binding to the activated cell and cholesterol efflux.

In this study, we demonstrate that AIBP clearly binds to TLR4 (but we do not exclude the possibility of AIBP binding to or affecting other receptors) and augments cholesterol efflux and disruption of lipid rafts, specifically in stimulated but not unstimulated microglia and macrophages. Because the first step in TLR4 signaling, homodimerization, occurs in lipid rafts, AIBP-mediated disruption of lipid rafts results in inhibition of the TLR4 inflammatory cascade. The AIBP-TLR4 binding and mechanism of action endow an unusual selectivity to the regulation of inflammatory receptors by changing cholesterol content in the plasma membrane (Tall and Yvan-Charvet, 2015). Treatment with beta-cyclodextrins to solubilize cholesterol is a common method to deplete cholesterol from the plasma membrane in cell culture experiments. Such depletion of cholesterol does result in inhibition of TLR4-mediated inflammatory signaling (Meng et al., 2010; Shridas et al., 2011). However, the physiologic mechanism of cholesterol removal from the cell involves the cholesterol transporters ABCA1 and ABCG1 and the extracellular cholesterol acceptors lipid-poor ApoA-I and the HDL, whose major protein is ApoA-I. Deficiency of cholesterol removal pathways results in overabundance of lipid rafts and stimulation of raft-associated signaling. Thus, there is a substantial increase in inflammatory gene expression in response to TLR4 ligands in *Abca1^{-/-}Abcg1^{-/-}* cells (Yvan-Charvet et al., 2008). The cholesterol acceptors HDL and ApoA-I stimulate cholesterol removal and reduce abundance of rafts, as well as inflammatory signaling (Mineo and Shaul, 2013; Murphy et al., 2008). Yet, these mechanisms of cholesterol efflux do not display any tissue or disease state selectivity, and the cellular cholesterol depletion by cyclodextrins, ApoA-I preparations, or LXR agonists, which upregulate ABCA1 and ABCG1 expression, are likely indiscriminate and yielding broad spectrum effects. In contrast, AIBP selectively directs the cholesterol efflux machinery to inflamed or cholesterol-overloaded cells, which serves to suppress inflammatory responses but not normal cell functioning.

In vivo neuraxial effect of i.t. AIBP on cholesterol export and TLR4 signaling.

The present work with i.t. AIBP remarkably confirms the in vitro cell culture effects of AIBP. The i.t. LPS acting through TLR4 receptors (as shown by the loss of i.t. LPS effects in TLR4 and MyD88 knockout mice (Stokes et al., 2013a; Stokes et al., 2013b) and following use of a TLR4 antagonist (Woller et al., 2016)) stimulated cytokine release and microglial and astrocyte activation. The transient protection by i.t. ApoA-I and an LXR agonist, provide in vivo support of our thesis of a cholesterol efflux-mediated mechanism of AIBP action, although we cannot exclude the contribution of other mechanisms. The demonstration that i.t. AIBP in fact significantly reduced TLR4 dimerization provides further support for the effects of AIBP being mediated by the proposed role on cholesterol efflux.

In vivo neuraxial effect of i.t. AIBP on facilitated pain states.

In the present study, i.t. AIBP had a selective effect upon the development of facilitated pain states. Thus, absent an effect upon phase 1 and phase 2 formalin, it is unlikely that the mechanism of action engages systems mediating acute nociception (Yaksh et al., 2001). Further, consistent with the proposed role of AIBP in regulating TLR4 signaling, the

facilitated pain models examined, i.t. LPS (Stokes et al., 2013b), phase 3 (but not phase 1 and 2) intraplantar formalin (Woller et al., 2016) and the cisplatin polyneuropathy (Park et al., 2014), all have been demonstrated through pharmacological antagonism or receptor / adaptor protein knockouts to have a pivotal role for TLR4 signaling. As such, the profile of the effects of i.t. AIBP matches the profile of those systems in which TLR4 signaling is pivotal. Our experiments with a mouse model of CIPN show the robust and long lasting (over 2 months) therapeutic effect of a single dose AIBP on tactile allodynia. This enduring effect raises the possibility of a disease-modifying effect. It is plausible that the prolonged effect of AIBP is due to altering a feedback inflammatory loop persisting in the spinal cord following cisplatin-induced injury.

Cellular target for i.t. AIBP.

As noted in these studies, we have shown that LPS evoked microglia and astrocyte activation and that this was reduced by i.t. AIBP. It is known that TLR4 protein is expressed on astrocytes and microglia and that their respective activation by LPS can yield cytokine release (Stokes et al., 2013b). The present work focused on the microglia to define TLR4 dimerization and cholesterol efflux. However, we have no reason to believe that other neuraxial cell types known to express TLR4, e.g., dorsal root ganglion neurons and astrocytes (Li et al., 2014; Liu et al., 2012; Tse et al., 2014), will not also show similar adaptive regulation of local lipid rafts by AIBP. Thus, while following LPS and intraplantar formalin there is an evident increase in microglial activation (Hoogland et al., 2015; Wu et al., 2004), such increases are rare in chemotherapy evoked neuropathies and effects upon DRG neurons and satellite cells, which express TLR4, may be more relevant (Li et al., 2014).

Role of endogenous AIBP in brain function.

AIBP is present in the CSF (Ritter et al., 2002) and has been indirectly implicated in regulation of brain function. A genome-wide meta-analysis identified *APOA1BP* (the gene encoding the AIBP protein) as a susceptibility locus for migraine (Anttila et al., 2013). A recent human study reports that *APOA1BP* variants leading to the loss of AIBP expression were found in a lethal neurometabolic disorder of early childhood (Kremer et al., 2016). Further studies are needed to explore the endogenous AIBP function.

Neuraxial delivery in developing therapeutics.

Systemic administration of analgesics is a preferred method. However, neuraxial drug delivery has a significant precedent, where the pathology has a spinal mechanism (as with pain and spasticity), and either the systemic agent does not have CNS bioavailability or the drug produces significant adverse events when delivered systemically at doses having a CNS effect (as with opiates). The morbidity associated with percutaneous injections is near zero when small gauge needles are employed (Corbey et al., 1997). There is an expanding development of spinally targeted drugs (Yaksh et al., 2017), particularly where the therapeutic has long lasting effects, as is suggested in the action of AIBP. While considerable work remains to be accomplished as regards safety and tolerability (Yaksh, 2011; Yaksh and Allen, 2004), the use of the intrathecal route to deliver AIBP, which, in the murine models, had no adverse events or morbidity and produced pain-ameliorating effects,

which endured for many weeks, represents a rational target for development as a therapeutic in long lasting facilitated pain states. Thus, for example, in patients receiving chemotherapy, there is a high prevalence of pain that last for periods of 3–6 months or more (Seretny et al., 2014). The effects noted for i.t. AIBP in the CIPN model showing long lasting therapeutic effects of a single dose AIBP are provocative.

EXPERIMENTAL PROCEDURES

Complete Experimental Procedures are in Supplement

Animals

All mouse experiments were conducted according to protocols approved by the IACUC of the University of California, San Diego. Behavioral studies were conducted with 2–4 month old male and female mice.

Cells

Thioglycollate-elicited peritoneal macrophages were harvested from C57Bl/6 mice and maintained in DMEM (Cellgro) supplemented with 10% heat-inactivated FBS (Omega Scientific) and 50 µg/ml gentamicin (Omega Scientific). Primary microglia were isolated from 2–3 week old C57Bl/6 mice as previously described (Gosselin et al., 2014). Immortalized microglial cell line BV-2 (Blasi et al., 1990) were maintained in DMEM supplemented with 5% FBS and 50 µg/ml gentamicin. Ba/F3 cells stably expressing TLR4-gfp, TLR4-flag and MD2 (Saitoh et al., 2004) were cultured in RPMI1640 (Invitrogen) containing 70 units/ml recombinant murine interleukin-3, 10% heat-inactivated FBS, 50 µg/ml gentamicin. HEK293 cells were cultured in DMEM supplemented with 10% FBS and 50 µg/ml gentamicin. THP-1 cells were maintained in RPMI-1640 supplemented with 10% FBS, 1% Pen/Strep and 2 mM L-glutamine, and differentiated into macrophages by a 72 hour incubation with 100 ng/ml PMA (Mukhamedova et al., 2016).

Yeast two-hybrid system

Interactions of the ectodomains of TLRs with AIBP were assessed by a yeast two-hybrid assay (BD Clontech, Palo Alto, CA), as described (Park et al., 2004).

Flow cytometry binding assay

Peritoneal macrophages and BV-2 microglia cells were blocked with TBS containing 1% BSA for 30 min on ice and incubated with either 2 µg/ml BSA or 2 µg/ml AIBP for 2 hours on ice. Cells were incubated with 1 µg/ml FITC-conjugated anti-His antibody (Abcam) for 1 hour at 4°C and analyzed using a FACSCanto II (BD Biosciences, San Jose, CA) flow cytometer.

TLR4 dimerization assays

The FACS method to measure TLR4 dimerization uses two TLR4 antibodies and isotype controls. MTS510 binds TLR4/MD2 only when it is a monomer (in TLR4 units) but not a dimer; SA15–21 binds to any cell surface TLR4 irrespective of its dimerization status (Akashi et al., 2003; Zanoni et al., 2016).

TLR4 dimerization was also assessed in Ba/F3 cells expressing TLR4-flag, TLR4-gfp and MD2, as described (Choi et al., 2013).

LPS, cyclodextrin, TAK-242, GW3965 and ApoA-I

In vitro experiments were conducted with Kdo2-LipidA (KLA; Avanti Polar Lipids), a well-characterized active component of LPS and a highly specific TLR4 agonist (Raetz et al., 2006); it is referred to in the text and figures as LPS. Our earlier studies have demonstrated that i.t. injections of KLA or ultra-pure LPS from *Escherichia coli* 0111:B4 (InvivoGen) produced identical allodynia responses in mice (Woller et al., 2016). In this study, we used for i.t. injections InvivoGen's LPS at 0.01 µg/µl or 0.1 µg/µl in 0.9% saline. The pharmaceutical grade beta-cyclodextrin CAVAMAX W7 PHARMA was from Wacker Chemie AG. The TLR4 inhibitor TAK-242 and the LXR agonist GW3965 were from Cayman Chemicals, and ultra-pure ApoA-I isolated from human plasma was from Academy Bio-Medical. Compounds for intrathecal injections were reconstituted in saline.

LPS binding assay

LPS binding to MD2 and AIBP was assessed in plate-based assay as described (Martínez-Sernández et al., 2016).

Isolation of lipid rafts

Lipid rafts were isolated using a detergent-free, discontinuous gradient ultracentrifugation method as in our earlier work (Fang et al., 2013).

Ex vivo and in vitro flow cytometry analysis of lipid rafts in myeloid cells and microglia

C57Bl/6 mice were intrathecally injected with saline or AIBP. Two hours later, mice were intrathecally injected with LPS. Fifteen min after LPS injection, spinal cords were harvested and fixed with 3.7% formaldehyde. Demyelinated single-cell suspensions were incubated with an anti-CD16/CD32 antibody (FcRγ blocker, BD Bioscience), followed by staining with an APC-conjugated CD11b antibody (BD Bioscience) and FITC-conjugated cholera toxin B (Sigma). Cells were analyzed using a FACSCanto II (BD Biosciences) flow cytometer. A similar assay was used to measure lipid raft abundance in cultured BV-2 microglia cells.

Cholesterol efflux assays

Cholesterol efflux assay was performed as previously described (Mukhamedova et al., 2016). No LXR agonists were used in cholesterol efflux experiments.

Recombinant AIBP

His-tagged AIBP was produced in a baculovirus/insect cell system to allow for posttranslational modification and to ensure endotoxin-free preparation and purified using a Ni-NTA agarose column eluted with imidazole.

Cisplatin treatment

Mice received intraperitoneal (i.p.) injections of cisplatin (2.3 mg/kg/injection; Spectrum Chemical MFG) on day 0 and day 2 to induce tactile allodynia. Between cisplatin injection days, lactated Ringer's solution (0.25 ml) was injected to maintain hydration and to protect the kidney and liver.

Mechanical allodynia

For testing, animals were placed in clear, plastic, wire mesh-bottomed cages for 45 min prior to the initiation of testing. Tactile thresholds were measured with a series of von Frey filaments (Semmes Weinstein von Frey Anesthesiometer; Stoelting Co.) ranging from 2.44–4.31 (0.04–2.00 g). The 50% probability of withdrawal threshold was recorded. The experimenter was blinded to the composition of treatment groups.

Formalin flinching

A metal band was placed around the left hindpaw of the mouse. After 1 hour acclimation with the metal band, the mouse received a single injection of intraplantar formalin (2.5%) to induce flinching. The movement of the metal band (mouse flinching) was detected by an automated device (Yaksh et al., 2001) for a period of 1 hour after delivery of formalin.

Statistical analyses

Results were analyzed using Student's t-test (for differences between 2 groups), one-way ANOVA (for multiple groups), or two-way ANOVA with the Bonferroni post hoc test (for multiple groups time course experiments), using GraphPad Prism. Differences between groups with $p < 0.05$ were considered statistically significant.

Supplementary Material

Refer to Web version on PubMed Central for supplementary material.

ACKNOWLEDGMENTS

We would like to thank Kelly Eddinger, B.S. for performing the thorough and systematic behavioral profile assessments.

This study was supported by grants NS102432 (Y.I.M. and T.L.Y.), NS099338 (T.L.Y. and M.C.), HL135737, HL136275, HL088093 (Y.I.M.), and T32AR064194 (S.A.W.) from the U.S. National Institutes of Health; SDG14710028 (S.-H.C.) from the American Heart Association; the Rheumatology Research Foundation (M.C.); and GNT1036352 from the National Health and Medical Research Council of the Australian Government (D.S.).

REFERENCES

- Agalave NM, Larsson M, Abdelmoaty S, Su J, Baharpoor A, Lundback P, Palmblad K, Andersson U, Harris H, and Svensson CI (2014). Spinal HMGB1 induces TLR4-mediated long-lasting hypersensitivity and glial activation and regulates pain-like behavior in experimental arthritis. *Pain* 155, 1802–1813. [PubMed: 24954167]
- Akashi S, Saitoh S. i., Wakabayashi Y, Kikuchi T, Takamura N, Nagai Y, Kusumoto Y, Fukase K, Kusumoto S, Adachi Y, et al. (2003). Lipopolysaccharide Interaction with Cell Surface Toll-like Receptor 4-MD-2: Higher Affinity than That with MD-2 or CD14. *J Exp Med* 198, 1035–1042. [PubMed: 14517279]

- Anttila V, Winsvold BS, Gormley P, Kurth T, Bettella F, McMahon G, Kallela M, Malik R, de Vries B, Terwindt G, et al. (2013). Genome-wide meta-analysis identifies new susceptibility loci for migraine. *Nat Genet* 45, 912–917. [PubMed: 23793025]
- Baranova I, Vishnyakova T, Bocharov A, Chen Z, Remaley AT, Stonik J, Eggerman TL, and Patterson AP (2002). Lipopolysaccharide down regulates both scavenger receptor B1 and ATP binding cassette transporter A1 in RAW cells. *Infect Immun* 70, 2995–3003. [PubMed: 12010990]
- Blasi E, Barluzzi R, Bocchini V, Mazzolla R, and Bistoni F (1990). Immortalization of murine microglial cells by a v-raf/v-myc carrying retrovirus. *J Neuroimmunol* 27, 229–237. [PubMed: 2110186]
- Cao L, Tanga FY, and Deleo JA (2009). The contributing role of CD14 in toll-like receptor 4 dependent neuropathic pain. *Neuroscience* 158, 896–903. [PubMed: 18976692]
- Choi S-H, Yin H, Ravandi A, Armando A, Dumlao D, Kim J, Almazan F, Taylor AM, McNamara CA, Tsimikas S, et al. (2013). Polyoxygenated cholesterol ester hydroperoxide activates TLR4 and SYK dependent signaling in macrophages. *PLoS One* 8, e83145. [PubMed: 24376657]
- Corbey MP, Bach AB, Lech K, and Frorup AM (1997). Grading of severity of postdural puncture headache after 27-gauge Quincke and Whitacre needles. *Acta Anaesthesiol Scand* 41, 779–784. [PubMed: 9241342]
- Fang L, Choi SH, Baek JS, Liu C, Almazan F, Ulrich F, Wiesner P, Taleb A, Deer E, Pattison J, et al. (2013). Control of angiogenesis by AIBP-mediated cholesterol efflux. *Nature* 498, 118–122. [PubMed: 23719382]
- Feldman P, Due MR, Ripsch MS, Khanna R, and White FA (2012). The persistent release of HMGB1 contributes to tactile hyperalgesia in a rodent model of neuropathic pain. *J Neuroinflammation* 9, 180. [PubMed: 22824385]
- Fessler MB, and Parks JS (2011). Intracellular lipid flux and membrane microdomains as organizing principles in inflammatory cell signaling. *J Immunol* 187, 1529–1535. [PubMed: 21810617]
- Gosselin D, Link VM, Romanoski CE, Fonseca GJ, Eichenfield DZ, Spann NJ, Stender JD, Chun HB, Garner H, Geissmann F, et al. (2014). Environment drives selection and function of enhancers controlling tissue-specific macrophage identities. *Cell* 159, 1327–1340. [PubMed: 25480297]
- Hoogland IC, Houbolt C, van Westerloo DJ, van Gool WA, and van de Beek D (2015). Systemic inflammation and microglial activation: systematic review of animal experiments. *J Neuroinflammation* 12, 114. [PubMed: 26048578]
- Huang PP, Khan I, Suhail MS, Malkmus S, and Yaksh TL (2011). Spinal botulinum neurotoxin B: effects on afferent transmitter release and nociceptive processing. *PLoS One* 6, e19126. [PubMed: 21559464]
- Hutchinson MR, Ramos KM, Loram LC, Wieseler J, Sholar PW, Kearney JJ, Lewis MT, Crysdale NY, Zhang Y, Harrison JA, et al. (2009). Evidence for a role of heat shock protein-90 in toll like receptor 4 mediated pain enhancement in rats. *Neuroscience* 164, 1821–1832. [PubMed: 19788917]
- Inoue K, and Tsuda M (2018). Microglia in neuropathic pain: cellular and molecular mechanisms and therapeutic potential. *Nat Rev Neurosci* 19, 138–152. [PubMed: 29416128]
- Joseph SB, Castrillo A, Laffitte BA, Mangelsdorf DJ, and Tontonoz P (2003). Reciprocal regulation of inflammation and lipid metabolism by liver \times receptors. *Nat Med* 9, 213–219. [PubMed: 12524534]
- Kremer LS, Danhauser K, Herebian D, Petkovic Ramadza D, Piekutowska-Abramczuk D, Seibt A, Muller-Felber W, Haack TB, Ploski R, Lohmeier K, et al. (2016). NAXE Mutations Disrupt the Cellular NAD(P)HX Repair System and Cause a Lethal Neurometabolic Disorder of Early Childhood. *Am J Hum Genet*.
- Li Y, Zhang H, Zhang H, Kosturakis AK, Jawad AB, and Dougherty PM (2014). Toll-like receptor 4 signaling contributes to Paclitaxel-induced peripheral neuropathy. *J Pain* 15, 712–725. [PubMed: 24755282]
- Liu T, Gao YJ, and Ji RR (2012). Emerging role of Toll-like receptors in the control of pain and itch. *Neurosci Bull* 28, 131–144. [PubMed: 22466124]

- Martínez-Sernández V, Orbegozo-Medina RA, Romarís F, Paniagua E, and Ubeira FM (2016). Usefulness of ELISA Methods for Assessing LPS Interactions with Proteins and Peptides. *PLoS One* 11, e0156530. [PubMed: 27249227]
- Meng G, Liu Y, Lou C, and Yang H (2010). Emodin suppresses lipopolysaccharide-induced pro-inflammatory responses and NF-kappaB activation by disrupting lipid rafts in CD14-negative endothelial cells. *Br J Pharmacol* 161, 1628–1644. [PubMed: 20726986]
- Miller RE, Belmadani A, Ishihara S, Tran PB, Ren D, Miller RJ, and Malfait AM (2015). Damage-associated molecular patterns generated in osteoarthritis directly excite murine nociceptive neurons through Toll-like receptor 4. *Arthritis & rheumatology (Hoboken, NJ)* 67, 2933–2943.
- Mineo C, and Shaul PW (2013). Regulation of signal transduction by HDL. *J Lipid Res* 54, 2315–2324. [PubMed: 23687307]
- Mukhamedova N, Brichacek B, Darwish C, Popratiloff A, Sviridov D, and Bukrinsky M (2016). Analysis of ABCA1 and Cholesterol Efflux in HIV-Infected Cells. *Methods Mol Biol* 1354, 281–292. [PubMed: 26714719]
- Murphy AJ, Woollard KJ, Hoang A, Mukhamedova N, Stirzaker RA, McCormick SPA, Remaley AT, Sviridov D, and Chin-Dusting J (2008). High-Density Lipoprotein Reduces the Human Monocyte Inflammatory Response. *Arterioscler Thromb Vasc Biol* 28, 2071–2077. [PubMed: 18617650]
- Ohtani Y, Irie T, Uekama K, Fukunaga K, and Pitha J (1989). Differential effects of alpha-, beta- and gamma-cyclodextrins on human erythrocytes. *Eur J Biochem* 186, 17–22. [PubMed: 2598927]
- Park HJ, Stokes JA, Corr M, and Yaksh TL (2014). Toll-like receptor signaling regulates cisplatin-induced mechanical allodynia in mice. *Cancer Chemother Pharmacol* 73, 25–34. [PubMed: 24162377]
- Park HJ, Stokes JA, Pirie E, Skahen J, Shtaerman Y, and Yaksh TL (2013). Persistent hyperalgesia in the cisplatin-treated mouse as defined by threshold measures, the conditioned place preference paradigm, and changes in dorsal root ganglia activated transcription factor 3: the effects of gabapentin, ketorolac, and etanercept. *Anesth Analg* 116, 224–231. [PubMed: 23223118]
- Park HS, Jung HY, Park EY, Kim J, Lee WJ, and Bae YS (2004). Cutting edge: direct interaction of TLR4 with NAD(P)H oxidase 4 isozyme is essential for lipopolysaccharide-induced production of reactive oxygen species and activation of NF-kappa B. *J Immunol* 173, 3589–3593. [PubMed: 15356101]
- Penning JP, and Yaksh TL (1992). Interaction of intrathecal morphine with bupivacaine and lidocaine in the rat. *Anesthesiology* 77, 1186–2000. [PubMed: 1466469]
- Raetz CRH, Garrett TA, Reynolds CM, Shaw WA, Moore JD, Smith DC, Jr., Ribeiro AA, Murphy RC, Ulevitch RJ, Fearn C, et al. (2006). Kdo2-Lipid A of Escherichia coli, a defined endotoxin that activates macrophages via TLR-4. *J Lipid Res* 47, 1097–1111. [PubMed: 16479018]
- Ritter M, Buechler C, Boettcher A, Barlage S, Schmitz-Madry A, Orso E, Bared SM, Schmiedeknecht G, Baehr CH, Fricker G, et al. (2002). Cloning and characterization of a novel apolipoprotein A-I binding protein, AI-BP, secreted by cells of the kidney proximal tubules in response to HDL or ApoA-I. *Genomics* 79, 693–702. [PubMed: 11991719]
- Saito O, Svensson CI, Buczynski MW, Wegner K, Hua XY, Codeluppi S, Schaloske RH, Deems RA, Dennis EA, and Yaksh TL (2010). Spinal glial TLR4-mediated nociception and production of prostaglandin E(2) and TNF. *Br J Pharmacol* 160, 1754–1764. [PubMed: 20649577]
- Saitoh S.-i., Akashi S, Yamada T, Tanimura N, Kobayashi M, Konno K, Matsumoto F, Fukase K, Kusumoto S, Nagai Y, et al. (2004). Lipid A antagonist, lipid IVa, is distinct from lipid A in interaction with Toll-like receptor 4 (TLR4)-MD-2 and ligand-induced TLR4 oligomerization. *Int Immunol* 16, 961–969. [PubMed: 15184344]
- Schmitz G, and Orso E (2002). CD14 signalling in lipid rafts: new ligands and co-receptors. *Curr Opin Lipidol* 13, 513–521. [PubMed: 12352015]
- Seretny M, Currie GL, Sena ES, Ramnarine S, Grant R, MacLeod MR, Colvin LA, and Fallon M (2014). Incidence, prevalence, and predictors of chemotherapy-induced peripheral neuropathy: A systematic review and meta-analysis. *Pain* 155, 2461–2470. [PubMed: 25261162]
- Sezgin E, Levental I, Mayor S, and Eggeling C (2017). The mystery of membrane organization: composition, regulation and roles of lipid rafts. *Nat Rev Mol Cell Biol* 18, 361–374. [PubMed: 28356571]

- Shridas P, Bailey WM, Talbott KR, Oslund RC, Gelb MH, and Webb NR (2011). Group \times secretory phospholipase A2 enhances TLR4 signaling in macrophages. *J Immunol* 187, 482–489. [PubMed: 21622863]
- Sorge RE, LaCroix-Fralish ML, Tuttle AH, Sotocinal SG, Austin JS, Ritchie J, Chanda ML, Graham AC, Topham L, Beggs S, et al. (2011). Spinal cord Toll-like receptor 4 mediates inflammatory and neuropathic hypersensitivity in male but not female mice. *J Neurosci* 31, 15450–15454. [PubMed: 22031891]
- Stokes JA, Cheung J, Eddinger K, Corr M, and Yaksh TL (2013a). Toll-like receptor signaling adapter proteins govern spread of neuropathic pain and recovery following nerve injury in male mice. *J Neuroinflammation* 10, 148. [PubMed: 24321498]
- Stokes JA, Corr M, and Yaksh TL (2013b). Spinal toll-like receptor signaling and nociceptive processing: regulatory balance between TIRAP and TRIF cascades mediated by TNF and IFN β . *Pain* 154, 733–742. [PubMed: 23489833]
- Sun Y, Yang M, Tang H, Ma Z, Liang Y, and Li Z (2015). The over-production of TNF- α via Toll-like receptor 4 in spinal dorsal horn contributes to the chronic postsurgical pain in rat. *J Anesth* 29, 734–740. [PubMed: 25895164]
- Tall AR, and Yvan-Charvet L (2015). Cholesterol, inflammation and innate immunity. *Nat Rev Immunol* 15, 104–116. [PubMed: 25614320]
- Tse KH, Chow KB, Leung WK, Wong YH, and Wise H (2014). Lipopolysaccharide differentially modulates expression of cytokines and cyclooxygenases in dorsal root ganglion cells via Toll-like receptor-4 dependent pathways. *Neuroscience* 267, 241–251. [PubMed: 24607321]
- Woller SA, Corr M, and Yaksh TL (2015). Differences in cisplatin-induced mechanical allodynia in male and female mice. *Eur J Pain*.
- Woller SA, Ravula SB, Tucci FC, Beaton G, Corr M, Isseroff RR, Soulika AM, Chigbrow M, Eddinger KA, and Yaksh TL (2016). Systemic TAK-242 prevents intrathecal LPS evoked hyperalgesia in male, but not female mice and prevents delayed allodynia following intraplantar formalin in both male and female mice: The role of TLR4 in the evolution of a persistent pain state. *Brain Behav Immun* 56, 271–280. [PubMed: 27044335]
- Wong SW, Kwon MJ, Choi AMK, Kim HP, Nakahira K, and Hwang DH (2009). Fatty Acids Modulate Toll-like Receptor 4 Activation through Regulation of Receptor Dimerization and Recruitment into Lipid Rafts in a Reactive Oxygen Species-dependent Manner. *J Biol Chem* 284, 27384–27392. [PubMed: 19648648]
- Wu Y, Willcockson HH, Maixner W, and Light AR (2004). Suramin inhibits spinal cord microglia activation and long-term hyperalgesia induced by formalin injection. *J Pain* 5, 48–55. [PubMed: 14975378]
- Yaksh TL (2011). Spinal Delivery and Assessment of Drug Safety In Fundamental Neuropathology for Pathologists and Toxicologists (John Wiley & Sons, Inc.), pp. 449–462.
- Yaksh TL, and Allen JW (2004). The use of intrathecal midazolam in humans: a case study of process. *Anesth Analg* 98, 1536–1545, table of contents. [PubMed: 15155302]
- Yaksh TL, Fisher C, Hockman T, and Wiese A (2017). Current and Future Issues in the development of spinal agents for the management of pain. *Curr Neuropharmacol* 15, 232–259. [PubMed: 26861470]
- Yaksh TL, Ozaki G, McCumber D, Rathbun M, Svensson C, Malkmus S, and Yaksh MC (2001). An automated flinch detecting system for use in the formalin nociceptive bioassay. *Journal of applied physiology (Bethesda, Md : 1985)* 90, 2386–2402.
- Yin K, Liao DF, and Tang CK (2010). ATP-binding membrane cassette transporter A1 (ABCA1): a possible link between inflammation and reverse cholesterol transport. *Mol Med* 16, 438–449. [PubMed: 20485864]
- Yvan-Charvet L, Welch C, Pagler TA, Ranalletta M, Lamkanfi M, Han S, Ishibashi M, Li R, Wang N, and Tall AR (2008). Increased inflammatory gene expression in ABC transporter-deficient macrophages: free cholesterol accumulation, increased signaling via toll-like receptors, and neutrophil infiltration of atherosclerotic lesions. *Circulation* 118, 1837–1847. [PubMed: 18852364]

- Zanoni I, Tan Y, Di Gioia M, Broggi A, Ruan J, Shi J, Donado CA, Shao F, Wu H, Springstead JR, et al. (2016). An endogenous caspase-11 ligand elicits interleukin-1 release from living dendritic cells. *Science* 352, 1232–1236. [PubMed: 27103670]
- Zhang M, Li L, Xie W, Wu JF, Yao F, Tan YL, Xia XD, Liu XY, Liu D, Lan G, et al. (2016). Apolipoprotein A-1 binding protein promotes macrophage cholesterol efflux by facilitating apolipoprotein A-1 binding to ABCA1 and preventing ABCA1 degradation. *Atherosclerosis* 248, 149–159. [PubMed: 27017521]

Author Manuscript

Author Manuscript

Author Manuscript

Author Manuscript

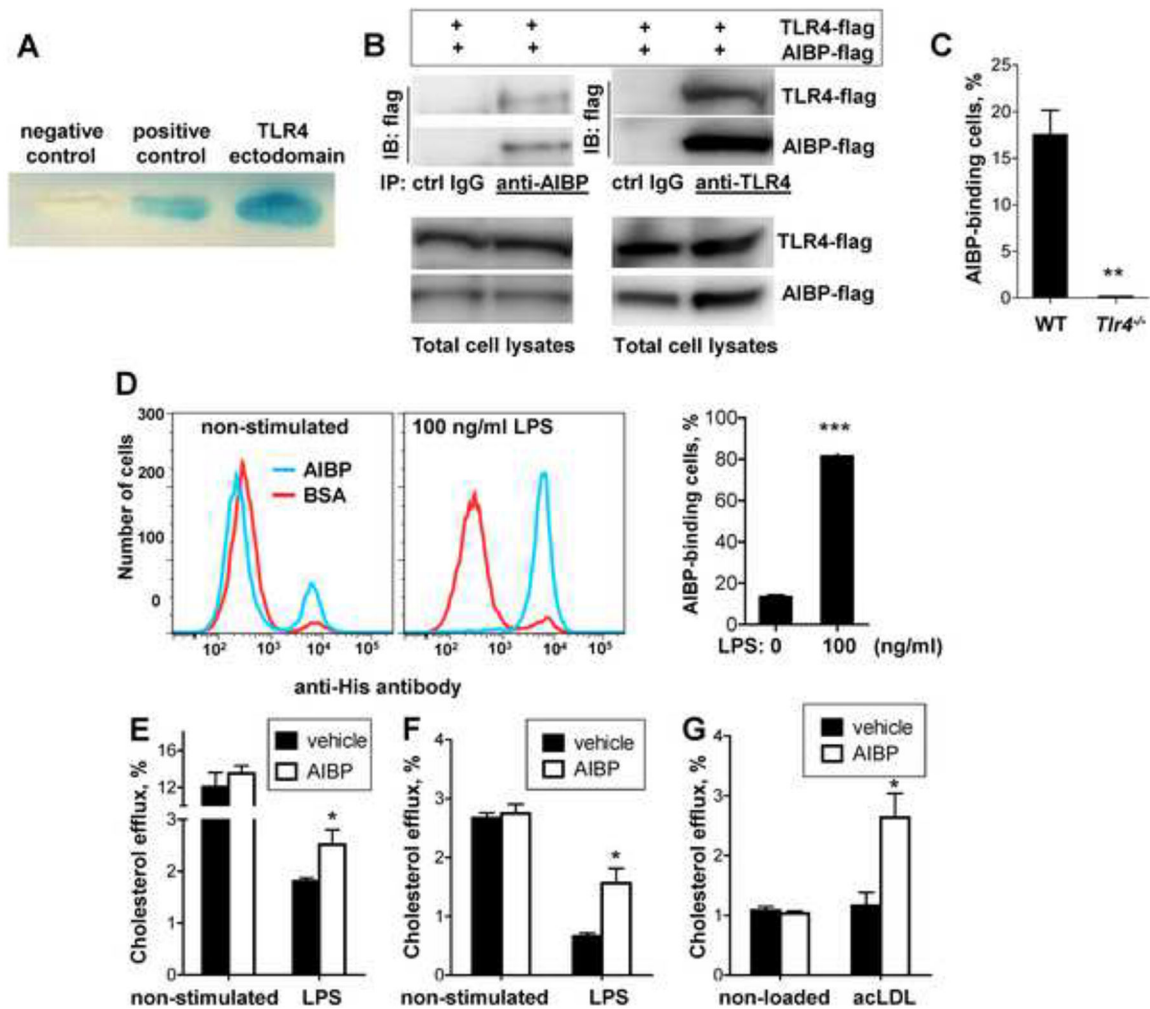


Figure 1. AIBP interaction with TLR4 and selective cholesterol efflux.

A, Yeast two-hybrid was performed with pB42AD-AIBP and pLexA-TLR4 ectodomain. The positive control was the yeast cell line EGY48/p80p-LacZ co-transfected with pLexA53 and pB42ADT; the negative control was the yeast cell line co-transfected with pLexA and pB42AD. **B**, HEK293 cells were co-transfected with the flag-tagged TLR4 ectodomain and flag-tagged AIBP. AIBP from cell lysates were pulled down with either anti-AIBP antibody, anti-TLR4 antibody or respective isotype control IgG. Blots of the pull-down or total cell lysates were probed with an anti-flag antibody. **C**, Peritoneal elicited macrophages from WT and *Tlr4*^{-/-} mice were incubated for 2 hours on ice with 2 μ g/ml BSA or 2 μ g/ml AIBP (with a His-tag) and then subjected to a flow cytometry analysis with a FITC-conjugated anti-His antibody. **D**, BV-2 cells were stimulated with 100 ng/ml LPS for 15 min, placed on ice, and 2 μ g/ml AIBP (His-tagged) or BSA were added for 2 hours, and cells were subjected to a flow cytometry analysis with a FITC-conjugated anti-His antibody. Mean \pm SEM; n=4; ***, p<0.001 (Student's t-test). **E**, Primary brain microglia cells were loaded with ³H-cholesterol, equilibrated and then sequentially incubated with 0.2 μ g/ml AIBP or BSA for 1 hour and 100 ng/ml LPS for 1 hour in complete medium. Cholesterol efflux was measured as described in Methods. Mean \pm SEM; n=3–5; *, p<0.05 (Student's t-test). **F**,

Human THP-1-derived macrophages were loaded with ^3H -cholesterol, equilibrated and incubated for 24 hours with 3 $\mu\text{g}/\text{ml}$ ApoA-I and 0.1% BSA, in the presence or absence of 0.2 $\mu\text{g}/\text{ml}$ AIBP. LPS (10 $\mu\text{g}/\text{ml}$) was added during equilibration and efflux incubations. Mean \pm SEM; n=4; *, p<0.05 (Student's t-test). **G**, Human THP-1-derived macrophages were loaded with acetylated LDL (acLDL; 50 $\mu\text{g}/\text{ml}$) and ^3H -cholesterol, equilibrated and incubated for 24 hours with 3 $\mu\text{g}/\text{ml}$ ApoA-I and 0.1% BSA, in the presence or absence of 0.2 $\mu\text{g}/\text{ml}$ AIBP. Cholesterol efflux was measured as described in Methods. Mean \pm SEM; n=4; *, p<0.05 (Student's t-test). See also Figure S1A.

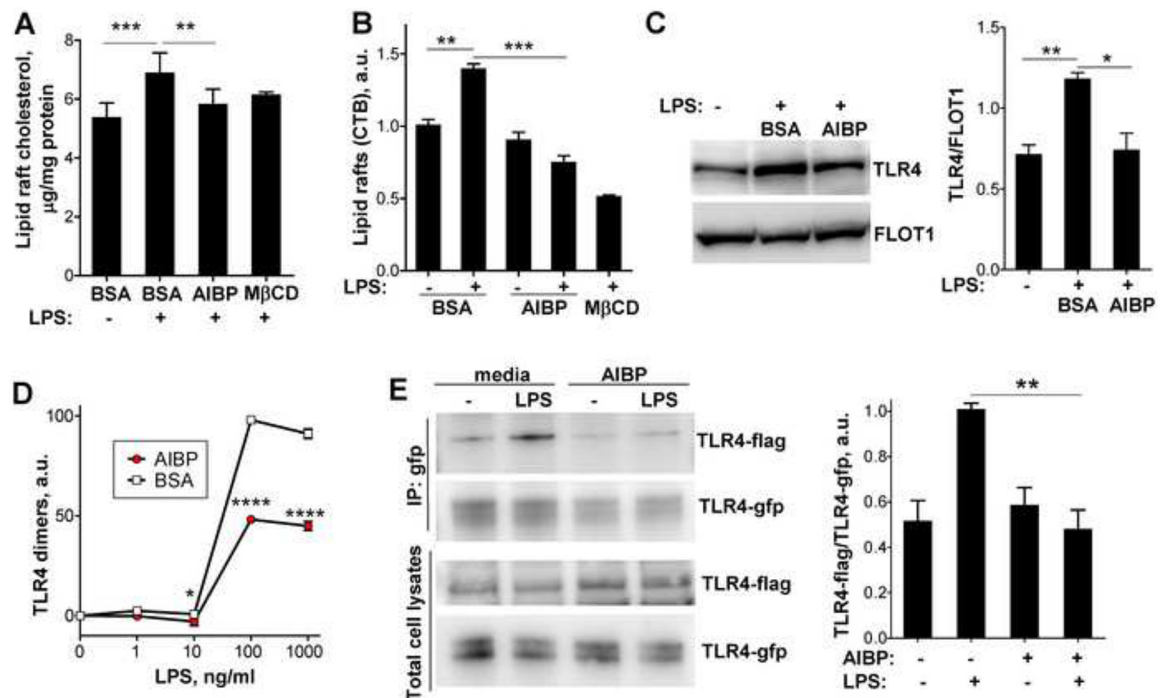


Figure 2. AIBP disrupts lipid rafts and inhibits TLR4 dimerization.

A-C, BV-2 cells were incubated for 2 hours with vehicle (0.1% BSA) or 0.2 μ g/ml AIBP (in 0.1% BSA) in serum-containing medium and stimulated with 10 ng/ml LPS for 10 min. **A**, Content of free cholesterol in isolated raft fractions was normalized to total cell protein. Mean \pm SEM; n=6 for first 3 columns; ***, p<0.001; **, p<0.01 (repeated measures ANOVA; raft isolation was performed for a single replicate of all samples per day); n=3 for M β CD. Mean \pm SEM; n=3; ***, p<0.001; **, p<0.01 (one-way ANOVA). **B**, Content of CTB-positive lipid rafts was measured in a flow cytometry assay. **C**, TLR4 occupancy in isolated lipid rafts was tested in western blot. Mean \pm SEM; n=3; **, p<0.01; *, p<0.05 (one-way ANOVA). **D**, BV-2 cells were preincubated for 2 h with 0.2 μ g/ml BSA or AIBP, followed by a 15 min incubation with LPS. Arbitrary numbers of TLR4 dimers were measured in a FACS assay with MTS510 and SA15–21 TLR4 antibodies as described in Methods. Mean \pm SD; n=3; p<0.05; ****, p<0.0001 (two-way ANOVA with Bonferroni post-test). **E**, Ba/F3 cells stably expressing TLR4-gfp, TLR4-flag and MD2 were incubated with serum-free media containing 50 μ g/ml HDL, in the presence or absence of 0.2 μ g/ml AIBP, and then stimulated with 10 ng/ml LPS for 20 min. Cell lysates were immunoprecipitated with an anti-GFP antibody and blots were probed with anti-flag and anti-GFP antibodies. Mean \pm SEM; n=4–6; **, p<0.01; Student's t-test. See also Figures S1B and S2.

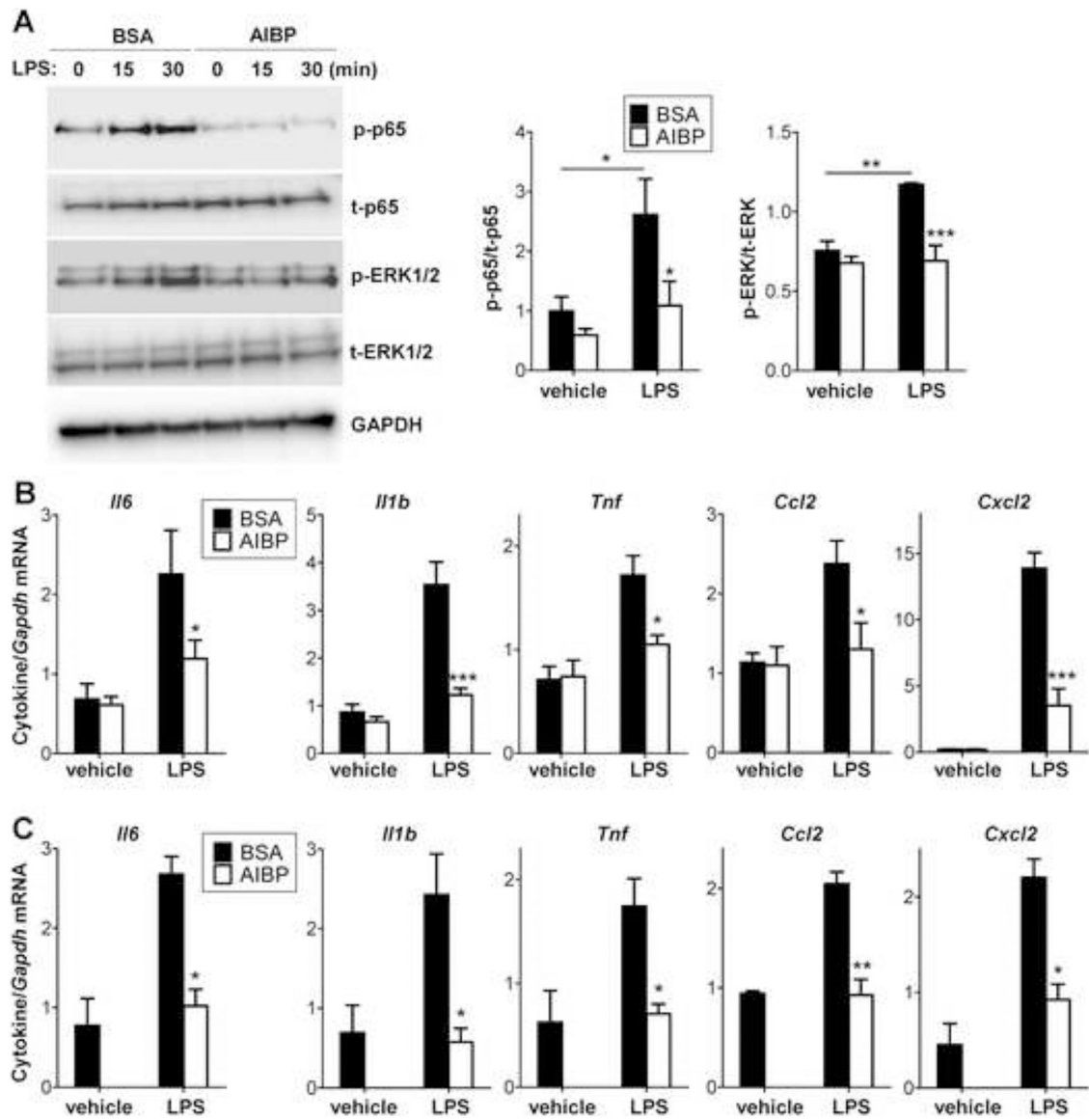


Figure 3. AIBP reduces inflammatory responses in microglia.

A-B, BV-2 cells were incubated for 2 hours with 0.2 $\mu\text{g/ml}$ BSA or AIBP in serum-containing medium and stimulated with 10 ng/ml LPS. p65 and ERK1/2 phosphorylation were tested after 30 min (**A**), and cytokine mRNA expression after 2 h of incubation (**B**). **C**, Primary mouse microglia (pooled from 5–6 mice per sample) were incubated for 2 hours with 0.2 $\mu\text{g/ml}$ BSA or AIBP in serum-containing medium and stimulated with 10 ng/ml LPS for 1 hour. Mean \pm SEM; $n=4-6$ for BV-2; $n=3$ for primary microglia experiments; *, $p<0.05$; **, $p<0.01$; ****, $p<0.0005$ (Student's t-test). Due to limited availability of primary cells, 'vehicle/AIBP' group was omitted. See also Figures S3 and S4A.

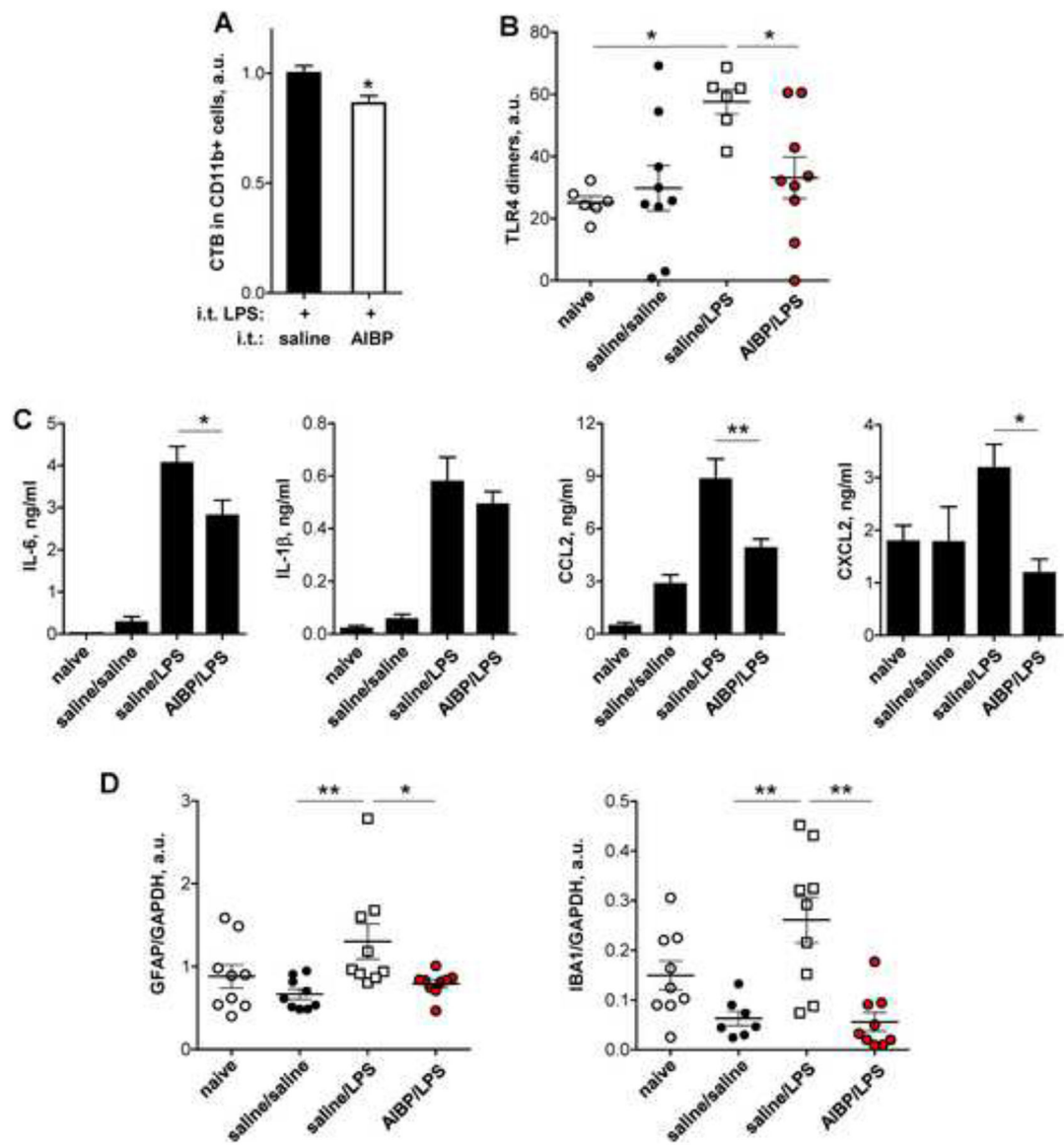


Figure 4. Intrathecal AIBP reduces lipid rafts and TLR4 dimerization in spinal myeloid cells, neuroinflammation, and glial activation.

A-B, Male mice were given an i.t. injection of AIBP (0.5 μ g/ 5 μ l) or saline (5 μ l); two hours later, all mice were given an i.t. injection of LPS (0.1 μ g/ 5 μ l) and were terminated 15 min later. **A**, Spinal cords were isolated, demyelinated, stained for CD11b and cholera toxin B (CTB) and subjected to a flow cytometry analysis. Mean \pm SEM; n=11; *, p<0.05 (Student's t-test). **B**, Demyelinated spinal homogenates were stained with MTS510, SA15–21 and isotype control antibodies, analyzed by flow cytometry, and levels of TLR4 dimers were calculated as described in Methods. Mean \pm SEM; n=6–9; *, p<0.05 (Newman-Keuls multiple comparison test). **C-D**, Male mice were given an i.t. injection of AIBP (0.5 μ g/ 5 μ l) or saline (5 μ l); two hours later, all mice were given an i.t. injection of LPS (0.1 μ g/ 5 μ l) and were terminated 4 hours later. Naïve mice were used as a negative control. **C**, CSF was isolated and tested in ELISA for the levels of inflammatory cytokines. Mean \pm SEM; n=8–11; *, p<0.05; **, p<0.01 (one-way ANOVA with Bonferroni's multiple comparison test).

Levels of TNF α in these samples were below detection limit. **D**, Lumbar spinal cord was isolated and analyzed in western blot for expression of GFAP and IBA1 (see Fig. S5). Mean \pm SEM; n=7-9; *, p<0.05; **, p<0.01 (non-parametric Kruskal-Wallis test with Dunn's multiple comparison test). See also Figures S4B and S5.

Author Manuscript

Author Manuscript

Author Manuscript

Author Manuscript

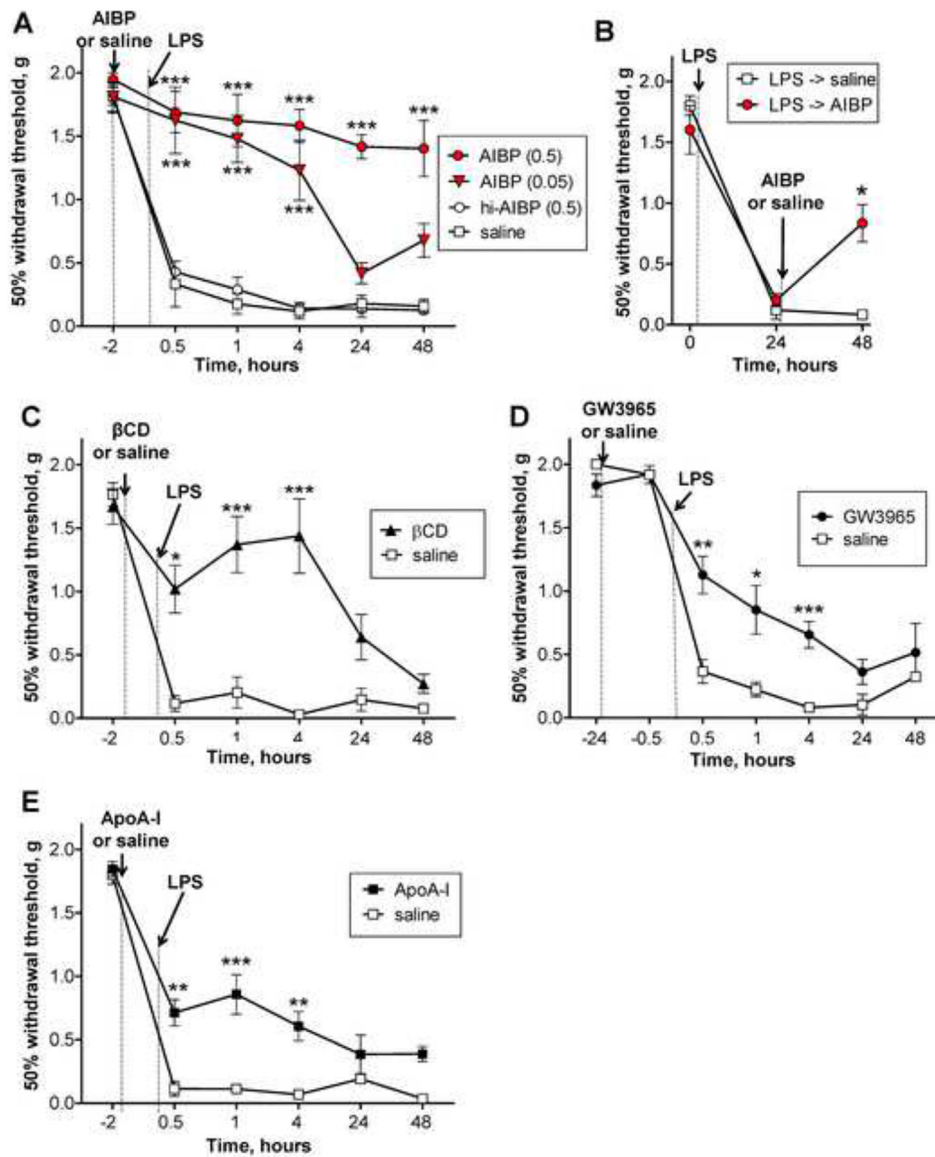


Figure 5. Intrathecal AIBP prevents and reverses LPS-induced allodynia.

A, Following baseline von Frey threshold testing, male mice were given an i.t. injection of AIBP (0.05 $\mu\text{g}/5\ \mu\text{l}$, $n=4$; or 0.5 $\mu\text{g}/5\ \mu\text{l}$, $n=6$), heat-inactivated AIBP (hi-AIBP; 0.5 $\mu\text{g}/5\ \mu\text{l}$; $n=6$), or saline (5 μl ; $n=6$). **B**, Following baseline von Frey threshold testing, male mice were given i.t. LPS (0.1 $\mu\text{g}/5\ \mu\text{l}$). Twenty-four hours later, mice received i.t. AIBP (0.5 $\mu\text{g}/5\ \mu\text{l}$; $n=4$) or saline (5 μl ; $n=4$). **C-E**, Following baseline von Frey threshold testing, male mice were given an i.t. injection of: **C**, beta-cyclodextrin (βCD ; 5 μl of 10% solution in saline; $n=4$) or saline (5 μl ; $n=4$; same group as used in panel A); **D**, the LXR agonist GW3965 (0.1 $\mu\text{g}/5\ \mu\text{l}$; $n=10$) or saline (5 μl ; $n=6$); or **E**, ApoA-I (5 $\mu\text{g}/5\ \mu\text{l}$; $n=10$) or saline (5 μl ; $n=6$). Two hours (**C** and **E**) or 24 hours (**D**) later, all mice were given an i.t. injection of LPS (0.1 $\mu\text{g}/5\ \mu\text{l}$) and tested over time for tactile allodynia. Mean \pm SEM; *, $p<0.05$; **, $p<0.01$; ***, $p<0.001$; ****, $p<0.0001$ (**A, C-E**: two way ANOVA with Bonferroni post-test; **B**: Student's *t*-test for the 48 hour time point only). See also Figure S6.

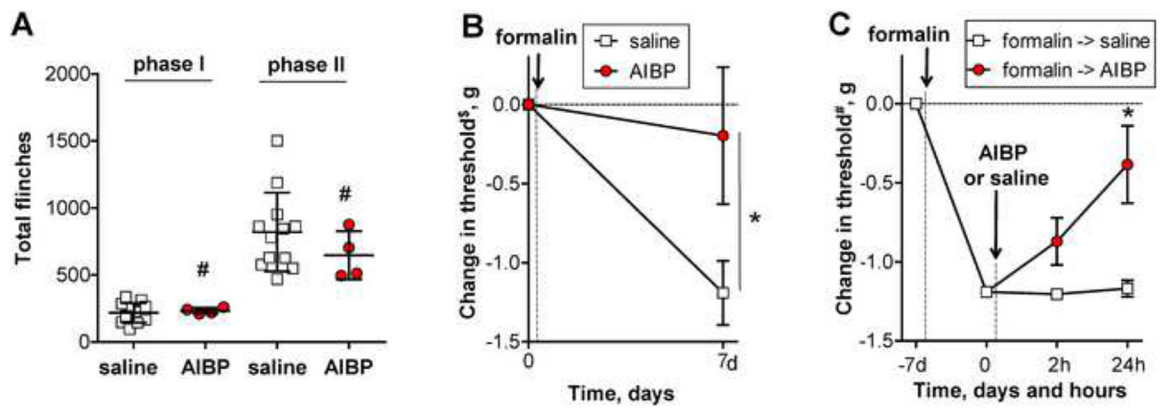


Figure 6. Intrathecal AIBP prevents and reverses i.t. LPS- and intraplantar formalin-induced allodynia.

A-B. Following baseline von Frey threshold testing, male mice were given an intraplantar injection of formalin in one hind paw. **A.** The graph shows total numbers of hind paw flinches in phase I (1–9 min) and phase II (10–50 min). Mean±SD; n=4–12 per group; #, non-significant, $p>0.05$ (Student's t-test). **B.** The graph shows $^{\$}$ baseline-normalized changes in the withdrawal threshold in the ipsilateral paw. Mean±SEM; n=4–12 per group; *, $p<0.05$ (Student's t-test for the 7 day time point only). **C.** In a group of animals different from those used in panels A and B, von Frey readings were $^{\#}$ normalized at the 7th day post-formalin and the mice received i.t. AIBP (0.5 μ g/ 5 μ l) or saline (5 μ l). Mean±SEM; n=4 per group; *, $p<0.05$ between 0 and 24 hours (repeated measures one-way ANOVA with Bonferroni post-test).

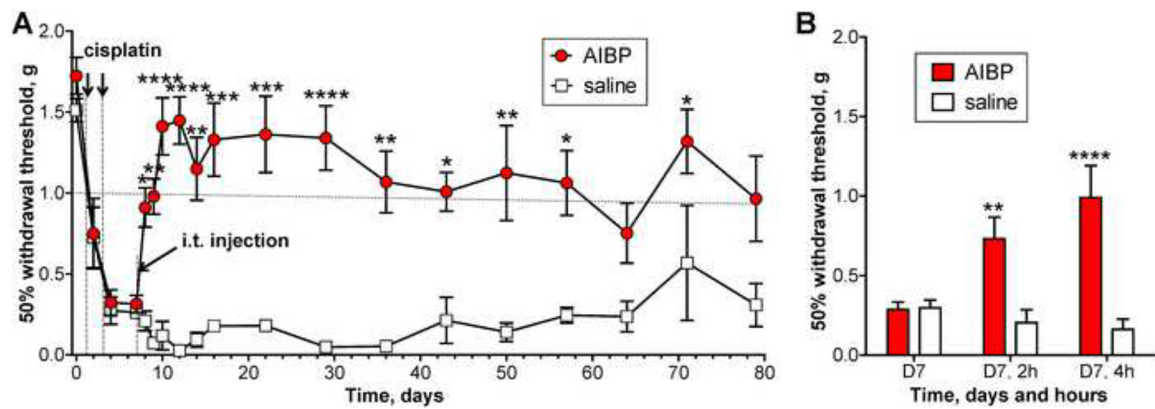


Figure 7. Intrathecal AIBP reverses established cisplatin-induced allodynia.

A, Male mice received 2 i.p. injections of cisplatin (2.3 mg/kg) over a period of 3 days to establish allodynia. On day 7, mice were treated with i.t. AIBP (0.5 μ g/ 5 μ l) or saline (5 μ l). Combined data from 2 independent experiments. **B**, The graph presents, in a different time scale, the experiment shown in panel A. Mice were tested on day 7 (after start of cisplatin treatment), before and 2 and 4 hours after i.t. AIBP and saline. Overall numbers of animals per group were on days 0–22: n = 17 (AIBP) and 12 (saline); days 29–79: n = 8 (AIBP) and 3 (saline). Mean \pm SEM. *, p<0.05; **, p<0.01; ***, p<0.001; ****, p<0.0001 (two way ANOVA with Bonferroni post-test).